Materials Science-Poland, *Vol. 27*, *No. 1*, *2009*

The effect of electromagnetic stirring on the microstructure and corrosion of mischmetal modified AZ91D magnesium alloy

Y. X. JIN[1, 2], L. HUA[2*], X. XU[2], Q. PENG[2]

[1]School of Materials Science and Engineering, Taiyuan University of Technology, 030024 Taiyuan PR China

[2]School of Materials Science and Engineering, Wuhan University of Technology, 430070 Wuhan, PR China

The microstructure and corrosion behaviour of mischmetal modified AZ91D magnesium alloy in the presence or absence of a rotating electromagnetic field have been investigated. The study suggests that the size and volume fraction of the β ($Mg_{17}Al_{12}$) phase in the alloy decreases as magnetic field intensity increases. The immersion test results show that the mass loss for the alloy solidified in the absence of a magnetic filed is always larger than that for the alloy solidified under magnetic field. The electrochemical corrosion experiments indicate that the corrosion potential of the alloys increases from –1.56 to –1.51 V, while the corrosion current density decreases from 6.31 to 1.58 $mA \cdot cm^{-2}$, and the charge transfer resistance increases from 3.17 to 11.32 $k\Omega \cdot cm^2$ as the excitation voltage increases from 0 to 120 V. The enhancement of the corrosion resistance is attributed to the grain refinement, and to the volume fraction reduction of the β ($Mg_{17}Al_{12}$) phase under a rotating electromagnetic field.

Key words: microstructure; corrosion; magnesium alloy; mischmetal

1. Introduction

Magnesium alloys exhibit an attractive combination of low density and high strength/weight ratio. Therefore, magnesium alloy parts are used in a variety of applications, such as in automotive, materials handling and aerospace equipment [1,2]. Among various magnesium alloys, the Mg–9Al–1Zn (AZ91) alloy is most widely used because of its excellent cast ability and mechanical properties. However, poor corrosive resistance of AZ91 magnesium alloy limits its potential use in further applications [3–5].

Achieving finer grain size generally leads to improved mechanical properties and structural uniformity of most metals and alloys [6]. Thus, a fine grain size in castings

*Corresponding author, e-mail: kingyaxu@yahoo.com.cn

is important for the service performance of cast products and is also important for the final properties of semifabricated products. Many grain-refining methods have been developed for magnesium alloy such as superheating, agitation, the additions of nucleant particles and solute elements [7–16]. Owing to the requirement for rapid cooling from the treatment temperature to pouring temperature, grain refinement by superheating is less practical for a large pot of melt on a commercial scale. Other shortcomings include excessive consumption of time and fuel/electricity and shortened life of the alloying vessels. The additions of nucleant particles can lead to obvious grain refinement but these particles are difficult to be consistently introduced into molten alloys. Generally, among the above-mentioned refinement techniques, electromagnetic agitation and the addition of rare earth elements to molten AZ91 alloys offer more practical advantages. Emadi et al. reported that adding Sr to AZ91D alloy significantly reduced its grain size from 225 to 75–150 μm [15]. Similar results were reported by other researchers[16]. However, a wide grain size distribution obtained in these investigations does not improve corrosion resistance. Thus, a suitable grain refiner for magnesium alloys is still elusive. The two general directions of resolving the grain refinement problem of magnesium alloys are therefore either to find a new additive that will perform the task or to significantly improve the efficiency of an existing casting process [6].

Electromagnetic processing of materials is an important technology developed by combining the magnetohydrodynamics and the casting engineering to improve the properties and performances of materials [17, 18]. Electromagnetic stirring (EMS) is one of the important magnetohydrodynamic applications, and is an alternative to the widespread high pressure die-casting and sand-casting methods for developing magnesium alloys. The use of the EMS is supported by a good quality of the casting alloy with fine non-dendritic structure, the lower shrinkage and uniform distribution of the grain size. Shijie Guo et al. reported that applying the electromagnetic vibration during the casting of the AZ80 magnesium alloy billet led to significant grain refinement [11]. However, their works mainly concentrated on the effects of an electromagnetic field on mechanical properties. Therefore, the present investigation is aimed at the fabrication of AZ91D magnesium alloy alloyed with mischmetal (Ce, La, Nd and other minor rare earth elements) and solidified by electromagnetic stirring generated with various excitation voltages. The main analysis is devoted to the microstructure and corrosion resistance.

2. Experimental

Material preparation and microstructural observation. Figure 1 shows the schematic diagram of a home-made electromagnetic stirring apparatus used in the present article. This apparatus is mainly made up of an electromagnetic stirrer, heating equipment, teeter chamber and smelting crucible. The rotating electromagnetic field is produced through the coil winding of asynchronous motor with excitation voltage ranging

from 0 to 120 V while maintaining the excitation frequency at 10 Hz. A resistance wire is placed in the gap space between the teeter chamber and refractor brick to heat the magnesium alloy. A graphite crucible for loading magnesium alloy is 60 mm in inner diameter, 70 mm in outer diameter, and 150 mm in height.

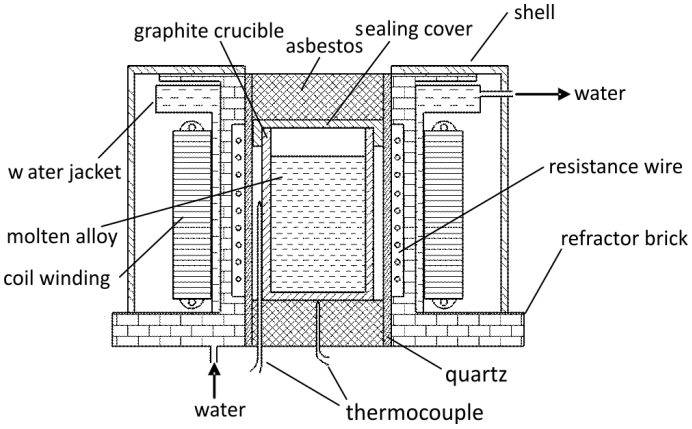

Fig. 1. Schematic diagram of the electromagnetic stirring apparatus

The chemical composition of the AZ91D magnesium alloy used in this study is as follows: Al – 9.1 wt. %, Zn – 0.85 wt. %, Mn – 0.27 wt. %, Mg – balance. Mischmetal (Ce – 50 wt. %, La – 20 wt. %, Nd – 10 wt. %, and balance other rare earths) is added at 1.0 wt. % levels. The AZ91D ingots were melted in an electric furnace and further refined at 730 °C under a protective gas mixture of 0.3% SF_6 and 99.7% CO_2. Mischemtal was added to the melt at 690 °C, held for 30 min. The melt was then transferred to the graphite crucible preheated to 200 °C. Finally, the current of the resistance wire was turned off at 640 °C, the excitation voltage of coil winding was turned on, and the molten alloy was cooled and solidified in the rotating electromagnetic field to ambient temperature.

Characterization of the grain size and qualitative analysis were conducted using an Olympus-BHM363U optical microscope (OM) and a JSM-5600LV scanning electron microscope (SEM) equipped with an Oxford energy dispersive X-ray (EDX) detector. The linear intercept method was used to measure the average grain size.

Immersion test. Immersion corrosion experiments were carried out to measure the corrosion rates of the modified alloys. The alloys were cut into rectangular specimens with dimensions of $10\times10\times2$ mm^3. All the specimens were polished successively with SiC paper up to 4000 grit and cleaned by ethanol. The specimens were immersed in a 5 wt. % NaCl aqueous solution saturated with $Mg(OH)_2$ for up to 5 days. The tests were conducted at room temperature. After immersion testing, corrosion products were removed by immersing the specimens in an aqueous solution of 20% CrO_3 + 1% $AgNO_3$.

Electrochemical tests. Specimens for electrochemical tests were cut into cubes with dimensions of 10×10×10 mm^3. The electrochemical tests were conducted in a 100 cm^3 submarine type cell using a typical three electrode fitting in which the working electrode was facing the counter electrode. The counter electrode was platinum, and a saturated calomel electrode (SCE) was used as reference. The working electrodes consisted of a cylindrical rod embedded in an epoxy resin to provide insulation, leaving 1.0 cm^2 alloy surface in contact with the electrolyte. Polishing was carried out on samples with SiC paper up to 4000 grit before measurements.

Potentiodynamic polarization curves for the investigated alloys in the 5 wt. % NaCl solutions saturated with $Mg(OH)_2$ at ambient temperature were determined using an CS300UA model electrochemistry analysis system at a scan rate of 1 $mV \cdot s^{-1}$. Before each polarization curve measurement, the sample was immersed in the test solution for 30 min to allow the open circuit potential to become stable.

The electrochemical impedance spectroscopy (EIS) measurements were carried out using an AUTOLAB PGSTA301 model electrochemical measuring device. The EIS measurements were obtained by applying a small-amplitude perturbation of 10 mV in a sine wave form, and by scanning the modulus of impedance and the phase shift over the frequency range from 10^{-2} Hz to 10^4 Hz. The electrode potential of each specimen was controlled at the relevant open circuit potential. The EIS data analysis was performed using the Zview software.

3. Results

3.1. Measured microstructures

Because microstructure determines the final properties of the alloy, an understanding of the microstructure formed is an essential part of the casting technology. Examination of the microstructures of the mischmetal modified AZ91D alloys shows that this is different when the alloys are solidified under different excitation voltages (Fig. 2). The view shows some agglomerate particles and acicular particles in the α magnesium matrix of alloy solidified in the absence of an electromagnetic field (Fig. 2a). A typical high multiple SEM image of the alloy for the EDX analysis is shown in Fig. 3, and composition of various compounds found in the alloy are listed in Table 1. The EDX result confirms that the agglomerate phases have compositions consistent with the $Mg_{17}Al_{12}$ phase. Acicular compounds are formed between Al and Ce or La, and contribute to the increased corrosion resistance of the alloy [3]. Hamana et al. reported that most of the rare earth elements added to Mg–Al alloys react with Al to form intermetallic compounds such as AlCe and Al_4La [19]. The result in the present study suggests a stoichiometric formula of Al_4(Ce, La). Thus the major elements (Ce and La) present in mischmetal satisfy the requirement of a modifying element as suggested by Ravi et al. [10].

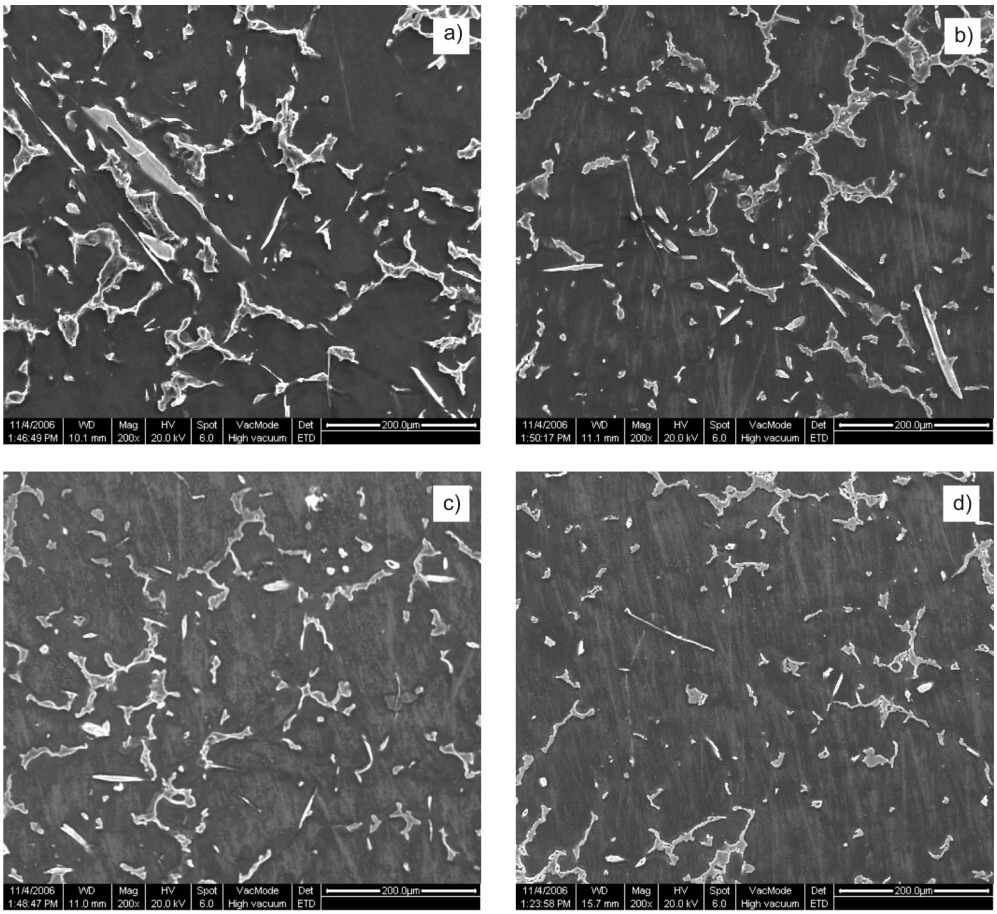

Fig. 2. SEM micrographs of mischmetal modified AZ91D magnesium alloys solidified under various excitation voltages: a) 0 V, b) 50 V, c) 80 V and d) 120 V

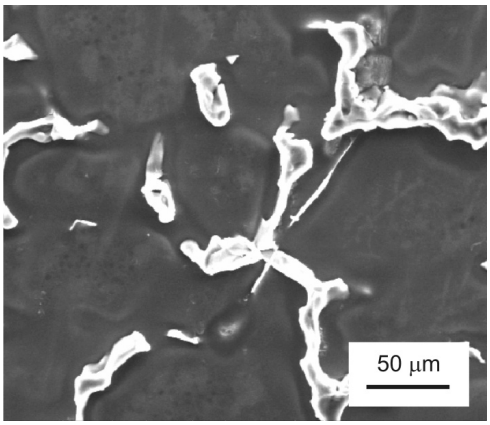

Fig. 3. High multiple SEM image of mischmetal modified AZ91D magnesium alloy solidified under the excitation voltage of 80 V

Table 1. Chemical compositions of phases of mischmetal modified AZ91D magnesium alloy solidified under the excitation voltage of 80 V (mole %)

Phase	Mg	Al	Zn	Mischmetal
$\beta(Mg_{17}Al_{12})$	56.32	38.28	5.4	
$Al_4(Ce, La)$	8.01	36.45	1.98	53.55

In the case of electromagnetic stirring casting, the grain refinement occurs, and the amount of irregular-shaped β ($Mg_{17}Al_{12}$) phase on grain boundaries decreases. When the exaction voltage is 50 V, the primary α magnesium grain size has no significant reduction, but agglomerate β ($Mg_{17}Al_{12}$) grain is obviously broken up and the volume fraction of $Al_4(Ce, La)$ phase increases (Fig. 2b). Increasing the intensity of the electromagnetic field results in a further grain refinement. Figure 3d shows the microstructure of the alloy specimen when the exaction voltage is increased to 120 V. Significant differences in grain size and homogeneity are observed. Due to a high intensity of the stirring, the structures of the alloy are greatly refined and become homogeneous. Large dendritic β grains are deformed into insular structure, and the grain boundaries are discontinuous.

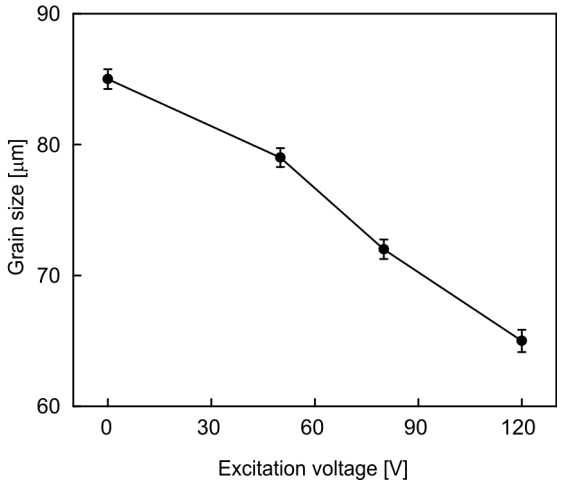

Fig. 4. Dependence of the α grain size of mischmetal modified AZ91D magnesium alloy on the excitation voltage

Figure 4 shows the relationship between the average grain size of the primary α magnesium and excitation voltage for the investigated alloys. The grain size gradually decreases from 85±0.7 μm to 65±0.8 μm on increasing the excitation voltage from 0 to 120 V. This confirms the modification of microstructure by the electromagnetic stirring during the solidification of the alloys. Considering that each grain is of a different size, the distribution of α magnesium grain size is investigated using an ImageTool software, and the results are listed in Table 2. Clearly, increasing the exci-

tation voltage results in a concentrated size distribution in the range of 40–80 μm. When the excitation voltage is 120 V, the percentage of α magnesium grain with the size range of 40–80 μm is 75%.

Table 2. Influence of electromagnetic field intensity on the distribution of α magnesium grain size

Excitation voltage [V]	< 40 μm	40–80 μm	> 80 μm
0	9%	36%	55%
50	11%	61%	28%
80	15%	63%	22%
120	18%	75%	7%

3.2. Immersion test

The mass loss curves recorded on the mischmetal modified alloys solidified under various excitation voltages are shown in Fig. 5. The mass loss of all the alloys increases with time but the values for the alloy solidified without magnetic filed are always larger than those for the alloys solidified under a magnetic field. Furthermore, the mass loss decreases with the increase in excitation voltage at any time between 1 and 5 days.

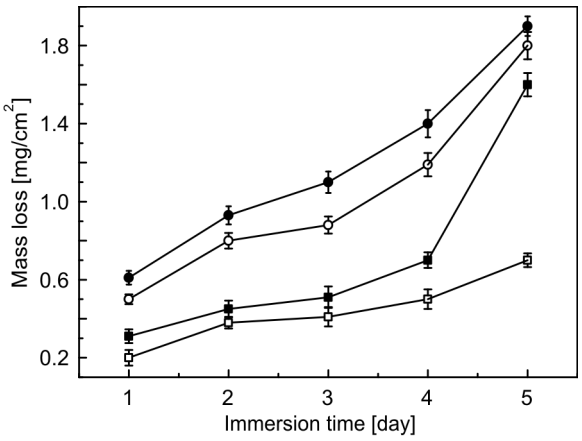

Fig. 5. Corrosion mass loss curves of the mischmetal modified AZ91D magnesium alloys solidified under various excitation voltages immersed in NaCl solution for up to 5 days: ● – 0 V, ○ – 50 V, ■ – 80 V, □ – 120 V

The effect of intensity of the electromagnetic field on the corrosion morphologies of the investigated alloys can be visualized from Fig. 6. The most outstanding characteristic of the morphology of the samples after being immersed in NaCl aqueous solution saturated with $Mg(OH)_2$ for 5 days is that all the corroded areas are adjacent to

the intermetallic precipitates, indicating that the corrosion is caused by the galvanic effect of the intermetallics. Figure 6a reveals that there existed serious general corrosion on the surface of the alloy solidified in the absence of an electromagnetic field. Moreover, some areas, perhaps originally surrounding the intermetallic precipitates, are completely corroded, and the intermetallic particles already fall off from there, leaving cavities in the α matrix. However, most areas of the alloys solidified in an electromagnetic field are not corroded or only a few areas are slightly corroded as shown in Fig. 6b–d. The results also indicate that upon increasing the intensity of the magnetic field, the surfaces of the samples remain more and more corrosion-free.

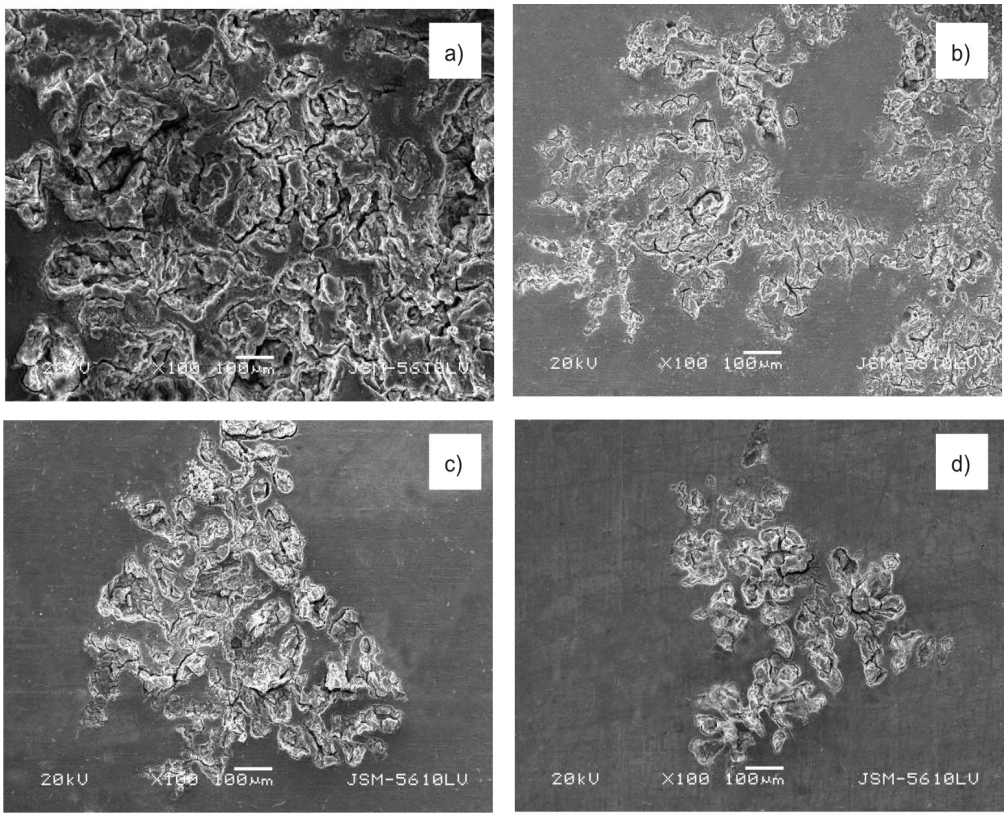

Fig. 6. SEM morphologies of corrosion surface of alloys solidified under various excitation voltages: a) 0 V, b) 50 V, c) 80 V and d) 120 V

3.3. Electrochemical tests

Figure 7 shows the potentiodynamic polarization curves of the investigated alloys. Obviously, the corrosion potential is shifted toward the active direction and the density of anodic current decreases rapidly at potentials just above –1.56 V for the alloy solidified in the absence of an electromagnetic field. It is noticed that the passivation

phenomena are invisible in the anodic regions of all the curves in the present study. In an earlier work by Mathieu et al., a plateau extending on a large anodic potential domain of the polarization curve in ASTM D1384 solution saturated with $Mg(OH)_2$ was obtained for the semi-solid cast AZ91D alloy [5]. The different results are mostly ascribed to the influence of the different corrosion media used in the experiments. In the present study, $Mg(OH)_2$ in the surface of magnesium alloy reacted with chloride anion in the NaCl solution, leading to the formation of soluble $MgCl_2$. The destructive effect of the chloride anion on the $Mg(OH)_2$ membrane makes the passivation phenomena invisible.

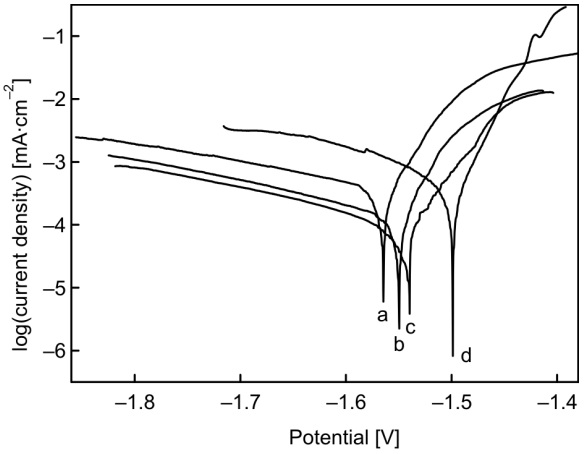

Fig. 7. Polarization curves of the mischmetal modified AZ91D magnesium alloys solidified under various excitation voltages: a) 0 V, b) 50 V, c) 80 V and d) 120 V

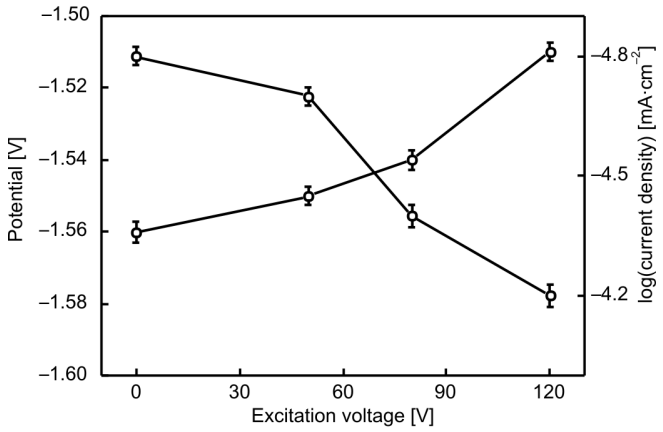

Fig. 8. Dependence of corrosion potential and corrosion current density of the mischmetal modified AZ91D magnesium alloys on the excitation voltage

Figure 8 shows the changes of corrosion potential and corrosion current density with the excitation voltage of the electromagnetic field. When the excitation voltage is

120 V, the corrosion potential is –1.51 V, being 3.52% higher than –1.56 V for the alloy solidified without electromagnetic field. The results indicate that the corrosion potential increases with the increase of the excitation voltage but at that time, the corrosion current density becomes reduced. Because the corrosion current density is directly proportional to the corrosion rate, the corrosion resistance of the mischmetal modified AZ91D magnesium alloy under the effects of rotating electromagnetic field is significantly enhanced.

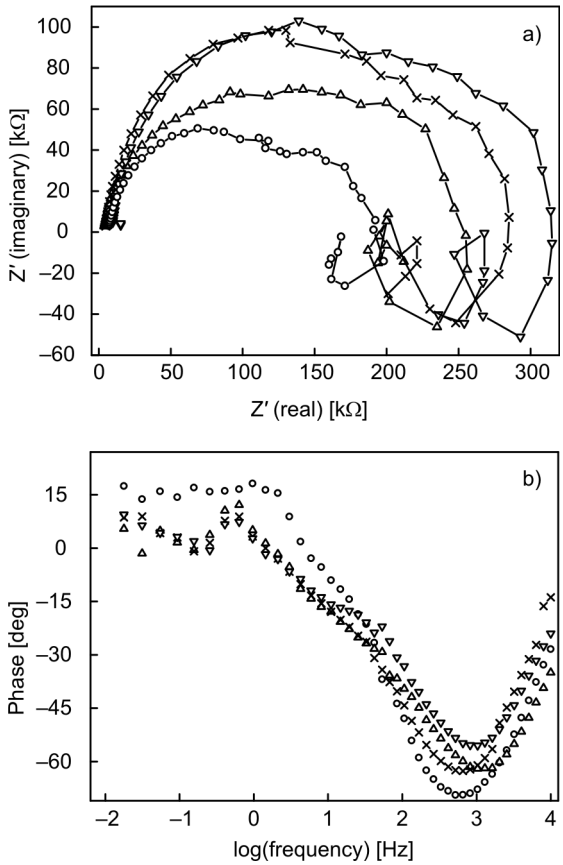

Fig. 9. EIS diagram of the mischmetal modified AZ91D magnesium alloys solidified under various excitation voltages in NaCl solution: a) Nyquist plots, b) Bode plots: ○ – 0 V, Δ – 50 V, × – 80 V, ∇ – 120 V

The EIS results of the present work are displayed in the form of Nyquist and Bode plots in Fig. 9. The Nyquist plots of the alloys at the open circuit potential display three arcs, which are capacitive arcs at both high and low frequency, and inductive arc at low frequency, respectively (Fig. 9a). The results are consistent with the prior work by Duan et al. [20]. It is believed that the corrosion process of magnesium alloy is irreversible, because the inductive arc only exists in the Nyquist plot of irreversible

electrode process. The impedance Bode plots display three extrema, including two maximum phase lags and one minimum phase lag (Fig. 9b). This implies that there exist three time constants (two capacitive responses and one inductive response) for mischmetal modified AZ91D magnesium alloys in NaCl solutions.

The corresponding equivalent circuit is shown in Fig. 10 which simulates the electrochemical behaviour of alloys in NaCl solution. The equivalent circuit contains elements corresponding to the solution resistance R_s, double-layer capacitance C, charge transfer resistance R_t, inductance component L, film surface resistance R_a, absorbing resistance R_c, and constant phase angle element CPE. The main electrochemical parameters derived from these experimental data are reported in Table 3.

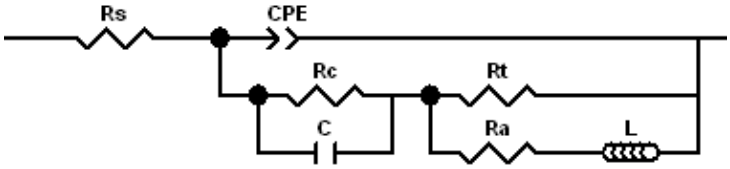

Fig. 10. Equivalent circuit of the mischmetal modified AZ91D magnesium alloys in NaCl solutions

Table 3. Equivalent circuit parameters of mischmetal modified AZ91D magnesium alloys solidified under various excitation voltages

Excitation voltage [V]	R_s [kΩ·cm^2]	C [μF·cm^{-2}]
0	3.17	3.14
50	4.28	2.56
80	6.41	1.52
20	11.32	1.33

The results show that the excitation voltage has a significant effect on the charge transfer resistance R_t and double-layer capacitance C. As the excitation voltage increases from 0 to 120 V, R_t increases from 3.17 to 11.32 kΩ·cm^2, but C decreases from 3.14 to 1.33 μF·cm^{-2}. The corrosion current density is inversely proportional to R_t. Therefore, the higher the R_t values, the more resistant the alloy is expected to be against corrosion. Moreover, the reduction of C indicates that the width of the electric double layer becomes broader. As a result, the hydrogen evolution reaction becomes slower, which is beneficial to the corrosion resistance enhancement of the alloys.

4. Discussion

4.1. The effect of an electromagnetic field on the microstructure of mischmetal modified AZ91D magnesium alloys

From the results obtained in our experiments, it can be seen that applying the electromagnetic stirring during solidification significantly refines the structure of the

mischmetal modified magnesium alloy. A review of the literature indicates that the structural refinement can be carried out by means of increased fluid flow induced by a magnetic field, an electric field, or a combination of both [11–14]. The effect is better appreciated with increasing superheat and solute element concentration. It is known that the molten undercooling during solidification increases under the influence of either an electric or a magnetic field [12]. This has been interpreted as the result of two competing processes: (1) fast growth of crystallites due to higher rate of mass transfer around each crystallite resulting in reduced superheating by accelerated release of latent heat of fusion and reduced nucleation, and (2) fast removal of heat along the solidification front, the effect of which is to enhance the tendency of the undercooling of the liquid metal and, hence, accelerate the process of nucleation.

In our experiments, the electromagnetic stirring was generated by application of a rotatory magnetic field in the molten metal. Under the effect of an alternative current of a certain frequency, the coil generates a time varying magnetic field in the melt, which in turn gives rise to an induced current in the molten metal. Therefore, the melt is subject to an electromagnetic body force (Lorentz force) caused by the interaction of the induced current and the magnetic field. The Lorentz force density consists of two parts, expressed as follows [11]

$$F = J \times B = -\nabla\left(\frac{1}{2}\mu B^2\right) + \frac{1}{\mu(B \cdot \nabla)B} \tag{1}$$

where B and J are the magnetic induction intensity and current density generated in the melt, and μ is the permeability of the melt. The first term on the right-hand side of Eq (1) is a rotational component which results in a forced convection and flow in the melt. The second term is potential forces balanced by static pressure of the melt, resulting in the formation of a convex surface and a decrease in the contacting pressure on the mold. Recent work by Fang et al. suggested that the electromagnetic body force of liquid metal in a rotating magnetic field is a sinusoidal function of the stirring time [18]. Therefore, the liquid metal in the rotating electromagnetic field experiences radial and tangential forces cyclically variable both in direction and magnitude.

Generally, a nucleus growth process can be divided into three phases: global growth, dendritic growth, and ripened rosette; and more nuclei imply a finer microstructure of the ingots [12]. According to the phase diagram of Mg–Al alloy, there should be a great amount of fine dispersed intermetallic particles such as $ZnAl_4$, $MnAl_6$, and $FeAl_3$ in a properly undercooled liquid metal being potential substratum for nucleation. When the electromagnetic pressure wave is imposed on the melt, some cavities form. Around the cavity, the melt is subject to a compressed stress; some atom clusters may form in this area. During the nucleation process, the atom clusters can easily attach to the particles to reduce the energy barrier for nucleation, thereby leading to the increased amount of nuclei. It was reported that the temperature field of the molten alloy with the rotating magnetic field was much lower and more uniform than that alloy without the magnetic field [11]. The merit of this uniform temperature field

is that the melt can be undercooled and nucleation can take place almost simultaneously in the mold resulting in an enlarged mushy zone. The subsequent result of this is that the microstructure of the alloy is fine and uniform. The structural differences shown in Fig. 2 are explained by the arguments put forward in the above discussion.

A molten alloy is a system consisting of atomic nuclei surrounded by electrons. The atomic nuclei make an irregular, thermal motion with a velocity. Under the electromagnetic field, they will revolve around the lines of the electromagnetic field; the radius of revolution and angular velocity are as follows [12]

$$r_c = \frac{mv_\perp}{|q|B} \tag{2}$$

where r_c is the revolution radius of the atomic nuclei in the electromagnetic field, q is the charge quantity of atomic nuclei, $v_\perp$ is the velocity in the vertical direction of the line of electromagnetic field, m is the mass of atomic nuclei, ω_c is the revolution angular velocity. Mg, Al, Zn and Ce ions are Mg^{2+}, Al^{3+}, Zn^{2+} and Ce^{3+}. Their radii of revolution and angular velocities are different because of the difference in m and q. Thus, a relative movement among Mg^{2+}, Al^{3+}, Zn^{2+} and Ce^{3+} will occur. As a result, the diffusion of rare earth elements in α matrix is strengthened which leads to an increase in the concentration of rare earth elements in the α matrix, and a decrease of the amount of $Mg_{17}Al_{12}$ phase on grain boundaries.

From the preceding discussion, it is clear that increasing the electromagnetic field intensity can result in a drastic forced convection of the melt and a relative movement among metal ions that will synchronously refine the structure and increase the content of rare earth elements within grains. This effect can be seen in Fig. 2.

4.2. The effect of an electromagnetic field on the corrosion behaviour of mischmetal modified AZ91D magnesium alloys

The manufacturing processes for magnesium alloy components have a great influence on the corrosion properties, since they determine the distribution of phases in the alloy. To some extent, the corrosion resistance of the AZ91D magnesium alloy depends on the morphology of the α magnesium and β phases. Numerous researchers investigated the role of the α magnesium and β grains in the corrosion, and have recognized that the β phase serves a dual purpose in the corrosion [3, 20]. When the α grain size is small, the gaps between the β precipitates are narrow and the distribution of the β phase is nearly continuous. In this case, the β phase acts as a barrier to corrosion. On the other hand, if the α grain size is large and the β phase is discontinuously distributed along the boundaries of the α phases, the β phase acts as a galvanic cathode because of the larger potential difference between the α and β phases. Moreover, the galvanic corrosion is intensified if the area ratio of cathode to anode is large.

In the alloy solidified without magnetic field, due to the larger size of the α and β grains, the β phase serves as an active cathode during corrosion. The galvanic corrosion inevitably occurs, owing to the galvanic current between the α and β phases. Applying electromagnetic stirring apparently decreases the grain size and also reduces the volume fraction of the β phase in AZ91D alloy by forming the Al_4(Ce, La) intermetallic compound which reduces the eutectic reaction between the α and β phases by consuming Al in the alloys. The change in the microstructure of the investigated alloy decreases the cathode-to-anode area ratio during corrosion. As a consequence, the galvanic current density of the alloy solidified under rotating electromagnetic field is obviously reduced. Some researchers also believed that the presence of the Al-rare earth intermetallic compound is responsible for the significantly enhanced corrosion resistance of the Mg–Al alloys [3, 9, 20]. Another factor for the corrosion resistance enhancement is that the grains are refined and the distribution of mischmetal composition and β phase is more uniform along the α grain boundaries. Even if a certain alloy grain is entirely corroded, the anti-corrosive mischmetal composition in the grain boundary can restrain the expansion of the corrosion process. In addition, there is not enough space in a single grain for a successful expansion of the corrosion pit. So the corrosion resistance of alloys solidified in the rotating electromagnetic field is enhanced.

5. Conclusion

By studying the fabrication and the properties of AZ91D magnesium alloy, alloyed with mischmetal, and solidified by electromagnetic stirring, the following conclusions can be drawn:

Electromagnetic stirring greatly refines the structure of the mischmetal modified alloys. The formation of the acicular Al_4(Ce, La) particles leads to a decrease in the volume fraction of $Mg_{17}Al_{12}$ phase. Increasing the electromagnetic stirring intensity leads to further grain refinement.

The corrosion resistance of the mischmetal modified AZ91D magnesium alloy solidified by electromagnetic stirring was significantly enhanced. The results of immersion test show that the mass loss for the alloy solidified in the absence of a magnetic field is always larger than the mass loss for the alloys solidified under a magnetic field. The electrochemical corrosion experiments indicate that the corrosion potential of the alloys increases, while the corrosion current density decreases, and the charge transfer resistance increases with the excitation voltage of the rotating electromagnetic field increasing from 0 to 120 V.

Acknowledgements

The authors acknowledge the financial support of the National Natural Science Foundation of China (Grant No. 50335060) and the Excellent Young Teacher Award of the Education Ministry of China (Grant No. [2002]383).

References

[1] HUTCHINSON C.R., NIE J.F., GORSSE S., Metall. Mater. Trans., A 36 (2005), 2093.
[2] WABUSSEG H., GULLO G.C., UGGOWITZER P.J., STEINHOFF K., KAUFMANN H., J. Mater. Sci., 37 (2002), 1173.
[3] SONG Y.L., LIU Y.H., YU S.R., ZHU X.Y., WANG S.H., J. Mater. Sci., 42 (2007), 4425.
[4] WAN Y., TAN J., SONG G.L., YAN C.W., Metall. Mater. Trans., A 37 (2006), 2313.
[5] MATHIEU S., RAPIN C., HAZAN J., STEINMETZ P., Corrosion Sci., 44 (2002), 2737.
[6] STJOHN D.H., QIAN M., EASTON M.A., CAO P., HILDEBRAND Z., Metall. Mater. Trans., A 36 (2005), 1669.
[7] YAO X.D., DAHLE A.K., DAVIDSON C.J., STJOHN D.H., J. Mater. Sci., 42 (2007), 9756.
[8] TAMURA Y., KIDA1 Y., TAMEHIRO H., KONO N., SODA H., MCLEAN A., J. Mater. Sci., 43 (2008), 1249.
[9] WANG Q.D., CHEN W.Z., DING W.J., ZHU Y.P., MABUCHI M., Metall. Mater. Trans., A 32 (2001), 787.
[10] RAVI M., PILLAI U.T.S., PAI B.C., DAMODARAN A.D., DWARAKADASA E.S., Metall. Mater. Trans., A 27 (1996), 1283.
[11] GUO S.J., LE Q.C., HAN Y., ZHAO Z.H., CUI J.Z., Metall. Mater. Trans., A 37 (2006), 3715.
[12] DONG J., CUI J.Z., YU F.X., BAN C.Y., ZHAO Z.H., Metall. Mater. Trans., A 35 (2004), 2487.
[13] MING X.G., BAO W.P., CUI J.Z., ZUO Y.B., Trans. Nonferrous Met. Soc. China, 13 (2003), 1270.
[14] MIZUTANI Y., KAWATA J., MIWA K., YASUE K., TAMURA T., SAKAGUCHI Y., J. Mater. Res., 19 (2004), 2997.
[15] EMADI D., GRUZLESKI J.E., TOGURI J.M., Metall. Mater. Trans., A 24 (1993), 1055.
[16] CLOSSET B., GRUZLESKI J.E., Metall. Mater. Trans., A 13 (1982), 945.
[17] GAO Y.L., LI Q.S., GONG Y.Y., ZHAI Q.J., Mater. Lett., 61 (2007), 4011.
[18] FANG C.F., ZHANG X.G., JI S.H., HAO H., JIN J.Z., Rare Metal Mater. Eng., 36 (2007), 170.
[19] HAMANA D., BOUCHEAR M., DERAFA A., Mater. Chem. Phys., 57 (1998), 99.
[20] DUAN H.Q., WANG S.L., CAI Q.Z., ZHANG S.C., WEI B.K., China Mech. Eng., 14 (2003), 1789.

Received 6 December 2008
Revised 19 December 2008